Using neutral atoms and standing light waves to form a calibration artifact for length metrology

J. H. Thywissen,[a)] K. S. Johnson, N. H. Dekker, A. P. Chu, and M. Prentiss
Department of Physics, Harvard University, Cambridge, Massachusetts 02138

(Received 29 May 1998; accepted 16 September 1998)

Beams of neutral metastable atoms can be patterned by spatially dependent deexcitation in a standing wave of laser light. Metastable atoms which hit a substrate transfer their internal energy (10–20 eV) to the surface and activate the formation of a durable carbonaceous resist from a vapor precursor. The resist can be used as an etch mask to transfer patterns into the substrate material. In this work, we report a recent experimental demonstration of this ''standing wave quenching'' (SWQ) patterning technique. We also present an analysis of the accuracy to which atom lithography and SWQ can form a periodic reference array for length metrology. We find that, with some modification of the experimental setup and parameters, the absolute period across a 1 mm^2 patterned area can be known to one part in 10^6.
[S0734-211X(98)12506-4]

I. INTRODUCTION

Neutral atom lithography has demonstrated parallel deposition of sub-100 nm lines and dots in periodic arrays.[1–3] In these techniques, an atom beam is patterned by a standing wave of laser light and then impinges upon an underlying substrate. In this article, we discuss the use of patterns formed by atom lithography as a periodic reference artifact, or ''nanoruler'', whose sub-micron period is known to sub-nanometer accuracy and precision. Such an artifact might be useful for accurate measurements of mm-scale distances or for calibration of a high-precision metrology tool.

Standing wave quenching (SWQ), the spatially dependent deexcitation of metastable atoms in a standing wave of laser light, has recently been demonstrated as a sub-100 nm atom lithographic patterning technique.[2] SWQ has several attractive features as the patterning step for a nanoruler: (1) the standing wave period is referenced to an atomic transition frequency; (2) the standing wave is directly retroreflected, which minimizes angular alignment errors; and (3) the waveguide-like nature of the atom-laser interaction makes the pattern periodicity insensitive to source properties. In Sec. II, we will explain SWQ in more detail and review recent experimental results; in Sec. III, sources of uncertainty in the period of the pattern will be discussed; in Sec. IV, we will compare this method with other methods and discuss future work.

II. METHOD AND RECENT RESULTS

Metastable argon (Ar*) and other metastable atoms[4] can be used to pattern a self-assembled monolayer resist[5,6] or to activate the growth of a carbonaceous resist material.[7–9] A subsequent etch step transfers the resist pattern to the substrate material, to form features with sizes as small as 20 nm.[9] Patterns have been transferred into Au, Si, SiO_2, Si_3N_4, and GaAs.[7–9]

The dissipation of the internal energy of Ar* (12 eV) can be initiated by a single IR photon before the atom reaches a surface. This process, known as optical ''quenching,'' converts a metastable atom, which contains sufficient energy to damage a resist or affect a surface, into a ground state atom, which is chemically inert.[5,7]

In SWQ, we use a periodic optical field to localize Ar* atoms on a nanometer length scale. The single infrared standing-wave field is used both to de-excite atoms from the metastable state to the inert ground state, and to confine the remaining metastable atoms in an optical potential.[10] The metastable atoms are quenched to the atomic ground state everywhere except in narrow regions around the nodes of the standing wave. Ar* atoms transmitted through the nodes release their energy at the surface to form a durable resist which subsequently serves as an etch mask [see Fig. 1(a)]. In a recent experiment, SWQ was used to pattern Si over an area of $\sim$0.5 mm^2 and form lines with widths as small as 65 nm [see Fig. 1(b)].[2]

In operation, the standing-wave field acts as a series of lossy waveguides for atoms. The light-induced potential confines atoms near the nodes of the standing wave, just as the index gradient in glass confines photons to the core of an optical waveguide. In the potential well formed by the standing wave, the ground state vibrational mode has a much lower loss rate than excited modes. After sufficient interaction with the standing wave light field, only metastable atoms in the ground vibrational mode remain. The product of the widths of the transverse position and momentum distributions of metastable atoms transmitted through each node can approach the limit stated by the Heisenberg uncertainty principle, $\Delta x \cdot \Delta p \geqslant \hbar/2$.

III. ERROR ANALYSIS

In this section we will examine the sources of error in the period of a pattern fabricated using atom lithography and SWQ. We will discuss the case of a grating patterned using a

a)Electronic mail: joseph@atom.harvard.edu

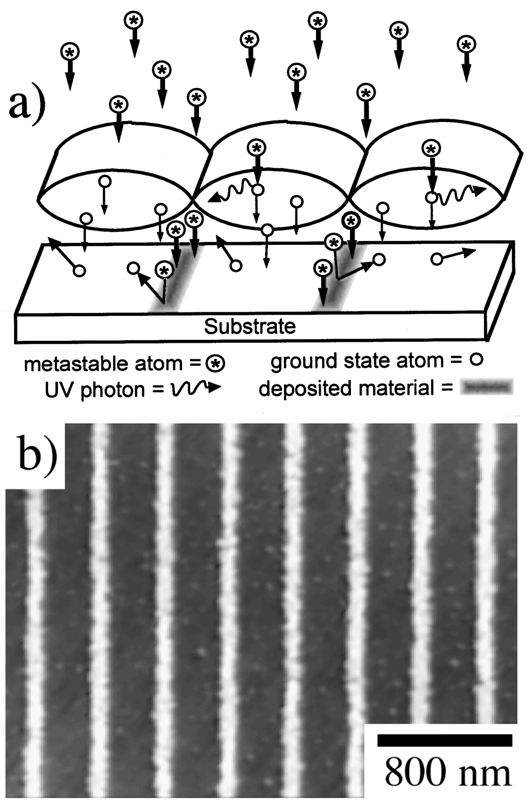

FIG. 1. (a) Schematic diagram of standing wave quenching (SWQ). Metastable atoms are optically quenched everywhere except in narrow regions around the nodes of the standing wave. An atom which is quenched dissipates its internal energy as an ultraviolet photon and returns to the inert atomic ground state. The transmitted metastable atoms interact with the surface and a background vapor precursor (not shown) to deposit a carbonaceous material. (b) Atomic force microscopy image of the pattern created by SWQ. The features (white in this image) etched into the Si ⟨110⟩ substrate had a height of 12 nm, had an average full width of 65 nm [as measured by a scanning electron microscopy (SEM)], and extended over an area of $\sim 0.5\ \mathrm{mm}^2$.

single standing wave, but the errors discussed also apply to a grid of dots patterned by a four-beam interference pattern.

In SWQ, features are formed beneath the nodes of the standing wave, which are nominally spaced by $\lambda/2$, where λ is the laser wavelength. As in all interferometric lithography (IL) methods,[11] the pattern is formed in a single exposure, such that there are no stepping errors. However, this method differs from most IL methods because the standing wave does not pattern the substrate directly. We will discuss both the errors in the mask periodicity (Secs. III A–III C) and the errors in the pattern transfer to the substrate via atoms (Secs. III D–III F).

A. Laser wavelength

The resonant wavelength of the $4s[3/2]_2^0 - 4p[5/2]_2$ quenching transition of argon is 801.6990 nm in vacuum, at a frequency of $3.739\,464 \times 10^{14}$ Hz.[12] Because exposures are performed in vacuum, the laser wavelength is not modified by refractive or pressure shifts. Thus, the accuracy to which

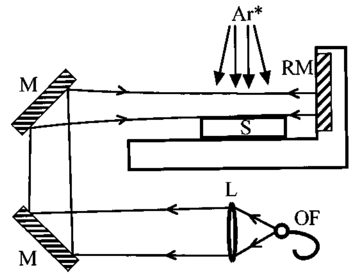

FIG. 2. Optical setup for standing wave quenching. M=mirror, OF=optical fiber, L=lens, RM=retroreflection mirror, Ar*=incident metastable argon atoms, and S=substrate. The outlines indicate the spatial extent of the laser light. Not to scale.

the wavelength is known is limited only by the accuracy with which the transition frequency can be measured, because the speed of light is a defined constant.

We use saturation spectroscopy[13] to lock the laser frequency to the $4s[3/2]_2^0 - 4p[5/2]_2$ resonant frequency. Laser spectroscopy is capable of extremely high precisions; without significant technical effort, we are able to determine the frequency of the laser to a precision of 1 MHz, which is approximately three parts in 10^9.

B. Standing wave angle

The period of a standing wave is $\lambda/2 \cos\theta$, where θ is the angle each beam makes with the plane of the substrate. For IL techniques which use the interference pattern of two beams directly to pattern a resist, θ must always be nonzero such that the light is incident on the substrate. Uncertainty in this angle dominates the uncertainty in the absolute period of the pattern formed.[14]

Since SWQ uses the standing wave as a *mask* for the atoms, the standing wave is above the substrate and can have $\theta \approx 0$ (see Fig. 2). In our experimental setup, we use the light from a single-mode optical fiber to form the standing wave. We align by retroreflecting the light through its original optical path to maximize its reinsertion back through the fiber. We measure the angular sensitivity of this procedure to be $\pm 50\ \mu$rad, which translates to a mask period which is $\lambda/2$ to roughly one part in 10^9.

C. Wave front aberrations

The standing wave is formed by a Gaussian beam whose minimum waist ($1/e^2$ intensity radius) is placed on the retroreflection mirror (see Fig. 2). This choice is made such that the interfering beams have the same profile. Nodes in the standing wave will have the same shape as the constant phase fronts of the interfering traveling waves. If atoms follow the nodes, just as light follows a curved optical fiber, then the nodal curvature will result in a systematic displacement of the pattern. If the curvature (and thus the displacement) changes across the patterned area, a systematic reduction in the period will occur.

The radius of curvature R of the wave fronts in a Gaussian beam at z away from the minimum waist is $R = z(1$

$+(z_0/z)^2)$, where λ is the wavelength of the light, $z_0 = \pi w_0^2/\lambda$ is the Rayleigh range, and w_0 is the minimum waist. Patterns are formed at approximately 1 cm from the retroreflection mirror across a length of 1 mm. If $w_0 = 1$ mm, then the curvature at $z = 1$ cm is 1.5 km, which results in a deviation from planar of $w_0^2/2R = 0.3$ nm at w_0 from the beam center. This deviation would increase by 0.03 nm across the 1 mm patterned area. Since only the increase in nodal displacement affects the period, the magnitude of this effect is only 0.03 nm, or three parts in 10^8, across the 1-mm-wide patterned area.

For smaller beam radii or larger patterned areas, this phase chirp of the pattern will be more significant. Also, angular errors not significant here (since they scale with the cosine of the wave front angle) may become important. However, since one can calculate the effect from the laser beam parameters, we could still predict the period to better accuracy than the magnitude of the effect.[15]

Diffraction from the clipping of the standing wave on the substrate (see Fig. 2) could also cause wave front distortion.[16] We have verified that the profile of a laser beam clipped at its edge (at $1/e^2$ of maximum intensity) is not significantly altered when viewed one Rayleigh range from the clip point. To avoid the effects of diffraction, one could ''preclip'' the Gaussian beam and then reimage the clipped profile above the substrate. Aberrations in mirrors and lenses would also distort wave fronts, but optics with figure and roughness on the nanometer scale are commercially available.

D. Substrate/mask alignment

The mirror which forms the standing wave determines the node positions in the standing wave: there must be a node on the mirror, and all nodes are spaced by $\lambda/2$. Thus if the mirror moves with respect to the substrate, the standing wave ''mask'' shifts, and the pattern can be blurred. To test the mechanical stability of our substrate mount, we used the retroflection mirror mount to hold one of two optical cavity mirrors. We found that the mount was sufficiently stiff that the relative motion would not significantly affect the fabricated feature size. Even if this motion were to broaden the features, the period would be unaffected.

If the mirror which retroreflects the quenching light is not perpendicular to the substrate, the average period on the substrate will be longer than the period of the mask by $1/\cos\theta$, where θ is the deviation from perpendicular of the substrate and mirror. In order to align this angle, we used a reflective substrate and the mirror as a corner cube for a HeNe alignment laser. Looking >1 m away, we could ensure that the angle is perpendicular to better than 1 mrad, such that the period is affected less than five parts in 10^7. This alignment procedure can easily be improved by using a larger distance or a smaller alignment beam.

E. Effects of incident atom angle

In principle, the incoming spatial and angular distribution of atoms affects only the coupling into the ground state vibrational mode of the standing wave, since the output spatial distribution is completely determined by the ground state mode. This is desirable for precise reproduction of the light mask, because the final pattern will be independent of source aberrations. In practice, some fraction of the excited vibrational states is still transmitted.

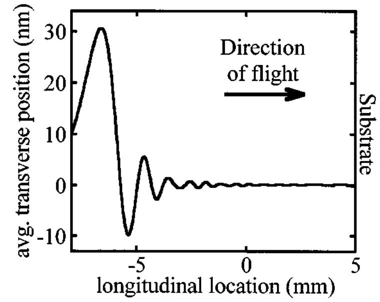

FIG. 3. Average transverse position, in nm, of a distribution of metastable atoms within a standing wave node, vs longitudinal location, in mm, relative to the center of the standing wave. In this example, Ar* atoms were incident on the standing wave with an average incident angle of +0.1 mrad. The atoms which initially oscillate about the node are quenched, such that the transmitted atomic distribution is centered to within $\lambda/3000$ of the node center. Laser parameters: 400 mW power, 35 MHz detuning above resonance, and 5 mm waist. Atomic beam parameters: uniform spatial distribution, 0.5 mrad angular spread, 0.1 mrad angular offset, and 800 m/s longitudinal velocity with $a \pm 13\%$ spread.

Figure 3 shows an example of the localization of an atomic wave packet within a standing wave node. Atoms with a 0.5 mrad angular spread and 0.1 mrad offset from perpendicular are incident on a standing wave with a waist of 5 mm, 400 mW total power, and a frequency 35 MHz above resonance.[17] As atoms enter the standing wave, they occupy multiple vibrational states and begin to oscillate. However, atoms in higher vibrational states are preferentially quenched, such that after sufficient interaction distance, all remaining metastable atoms are localized near the nodes. A substrate could be placed at +5 mm (see Fig. 3), where the atoms are centered to $\lambda/3000$, or 0.3 nm. This error is not cumulative, i.e., the offset of one wave packet does not offset the adjacent node's wave packet. Therefore if 0.1 mrad is the largest incident atomic angle across a pattern 1 mm in length, the error in the average period of the pattern will be three parts in 10^7.

The mean position of transmitted atoms that had larger initial angular offsets would deviate farther from the center of a node. However, higher angles lead to smaller transmissions because the atoms couple less well into the ground state, so high contrast patterns will appear only in the regions of high accuracy. Transverse laser cooling[18] allows the atoms to be incident at average angles of less than 0.1 mrad across a 1 mm^2 patterned area.

F. General issues when using a reference artifact

There are several error sources which apply to the use of any reference artifact: (1) measuring and stabilizing the temperature of the substrate; (2) minimizing the strain of the substrate due to clamping; (3) measurement uncertainty.

The period of the artifact must be corrected for the change in temperature between fabrication and measurement. The temperature of the substrate in our current apparatus is stabilized to ± 15 mK. We have patterned SiO_2 with a variety of etching techniques, and therefore it would be possible to etch patterns into, for instance, fused silica, which has a coefficient of expansion of $0.6\times 10^{-6}\ K^{-1}$. Thus a 15 mK uncertainty would correspond to a period uncertainty of less than one part in 10^8.

When affixing the substrate to a mounting surface, clamp-induced stress may distort the period of the pattern. Silicon and glasses have elastic modulae of $\sim$150 GPa. If a clamping force of less than 1 N is used at the ends of a substrate with a 10 mm$\times$1 mm cross section, a strain of less than one part in 10^6 would result.

Measuring the center of a particular line has a limited accuracy. The features formed in the SWQ experiment described in Sec. II were 65 nm wide; assuming the line could be split to one part in 20, the average period across a 1 mm patterned area could only be measured to three parts in 10^6. Also, after etching the patterns are not perfectly smooth, as shown in Fig. 1(b). Smoother and smaller lines[10] will make this measurement easier. Furthermore, measuring the distance between lines is limited by the degree to which perpendicular can be determined. Fabricating a grid of dots instead of lines would solve this problem if the axes of two dimensions in the grid are perpendicular to sub-mrad precision. Dot arrays have been fabricated with other atom lithographic schemes,[19] and fabrication of such a pattern is also possible with SWQ.

IV. CONCLUSIONS

SWQ is promising as a technique to produce periodic patterns whose absolute period is known to sub-nm accuracy. The strengths of the method include a period referenced to an atomic transition frequency, small alignment-induced errors, and insensitivity to source properties. Assuming we are limited by those errors which were estimated in Sec. III, SWQ can create a reference array whose average period is known to one part in 10^6 across 1 mm. Using this array as a calibration artifact with an accuracy of 1 ppm would be possible if an array of $\sim$20-nm-wide dots were fabricated in a rectilinear array.

An alternative patterning approach has been to use standing wave focusing (SWF),[1] an atom lithographic technique in which the standing light wave acts as an array of lenses for atoms, just as the standing wave acts as an array of waveguides for atoms in SWQ. The period of the standing wave is similarly referenced to an atomic transition, but there are several important differences: (1) small feature sizes in SWF require small laser spot sizes such that the wave front curvature (Sec. III B) would be more significant; (2) optimal focusing occurs near the center of the laser profile, which requires that the substrate clip the laser profile more significantly; (3) the line positions at the substrate depend upon the incoming atoms' angles, because images are formed in the Fourier plane of the standing wave lenses. Measurements of a pattern formed by SWF are currently in progress at the National Institute of Standards and Technology (NIST).[20]

Future work includes using SWQ to fabricate a structure with high expected accuracy, and then measuring the period of the pattern produced. Fabrication of an array of dots would eliminate errors due to nonperpendicular translation between lines. Finally, improvements to the technique such as smaller features, larger patterned area, and lower run times would facilitate fabrication and evaluation of these reference artifacts.

ACKNOWLEDGMENTS

This work was supported in part by the NSF (PHY 9312572). J. T. was supported by the Fannie and John Hertz Foundation; K. J. by an AT&T/Lucent Graduate Fellowship. The authors thank M. Schattenburg, J. Ferrera, T. Savas, and H. Smith for fruitful conversations. The authors also acknowledge their collaborators, K. Berggren and R. Younkin.

[1] G. Timp, R. E. Behringer, D. M. Tennant, J. E. Cunningham, M. Prentiss, and K. K. Berggren, Phys. Rev. Lett. **69**, 1636 (1992); J. J. McClelland, R. E. Scholten, E. C. Palm, and R. J. Celotta, Science **262**, 877 (1993); R. W. McGowan, D. M. Giltner, and S. A. Lee, Opt. Lett. **20**, 2535 (1995); U. Drodofsky, J. Stuhler, B. Brezger, Th. Schulze, M. Drewsen, T. Pfau, and J. Mlynek, Microelectron. Eng. **35**, 285 (1997); F. Lison, H.-J. Adams, D. Haubrich, M. Kreis, S. Nowak, and D. Meschede, Appl. Phys. B: Lasers Opt. **65**, 419 (1997).

[2] K. S. Johnson, J. H. Thywissen, N. H. Dekker, K. K. Berggren, A. P. Chu, R. Younkin, and M. Prentiss, Science **280**, 1583 (1998).

[3] J. H. Thywissen, K. S. Johnson, R. Younkin, N. H. Dekker, K. K. Berggren, A. P. Chu, M. Prentiss, and S. A. Lee, J. Vac. Sci. Technol. B **15**, 2093 (1997).

[4] The metastable rare gas atoms have the following energies: He*=20 eV, Ne*=17 eV, Ar*=12 eV, Kr*=10 eV, and Xe*=8 eV. Their natural lifetimes are $\geqslant$20 ms, which is much longer than their typical flight times.

[5] K. K. Berggren, A. Bard, J. L. Wilbur, J. D. Gillaspy, A. G. Helg, J. J. McClelland, S. L. Rolston, W. D. Phillips, M. Prentiss, and G. M. Whitesides, Science **269**, 1255 (1995).

[6] S. Nowak, T. Pfau, and J. Mlynek, Appl. Phys. B: Lasers Opt. **63**, 203 (1996); A. Bard *et al.*, J. Vac. Sci. Technol. B **15**, 1805 (1997).

[7] K. S. Johnson, K. K. Berggren, A. Black, C. T. Black, A. P. Chu, N. H. Dekker, D. C. Ralph, J. H. Thywissen, R. Younkin, M. Tinkham, M. Prentiss, and G. M. Whitesides, Appl. Phys. Lett. **69**, 2773 (1996).

[8] S. J. Rehse, A. D. Glueck, S. A. Lee, A. B. Goulakov, C. S. Menoni, D. C. Ralph, K. S. Johnson, and M. Prentiss, Appl. Phys. Lett. **71**, 1427 (1997).

[9] J. H. Thywissen, K. S. Johnson, N. H. Dekker, M. Prentiss, S. S. Wong, M. Weiss, and M. Grunze, J. Vac. Sci. Technol. B **16**, 1155 (1998).

[10] A. P. Chu, K. K. Berggren, K. S. Johnson, and M. Prentiss, Quantum Semiclassic. Opt. **8**, 521 (1996).

[11] G. Schmahl and D. Rudolph, *Progress in Optics XIV*, edited by E. Wolf (North-Holland, Amsterdam, 1976), p. 196 and references therein; E. H. Anderson, C. M. Horwitz, and H. I. Smith, Appl. Phys. Lett. **43**, 874 (1983).

[12] NIST Database for Atomic Spectroscopy, NIST Standard Reference Database **61**, July 1995.

[13] K. Simoda, *Introduction to Laser Physics* (Springer-Verlag, Berlin, 1991), pp. 148–165.

[14] Henry I. Smith (private communication).

[15] The effect of curved wave fronts in interferometric lithography was modeled by J. Ferrera, M. L. Schattenburg, and H. I. Smith, J. Vac. Sci. Technol. B **14**, 4009 (1996).

[16] The sample is positioned such that it clips the standing wave at its waist because the atoms begin to diffract once they are released from the optical potential.

[17] When the laser frequency is detuned above the atomic resonance, the light induces an electric dipole moment in the atoms. The potential energy of

the dipole in the electric field of the standing wave is quadratic about each node. For a review of atom optics and optical forces, see C. S. Adams, M. Sigel, and J. Mlynek, Phys. Rep. **240**, 143 (1994), and references therein.

[18]For a review of laser cooling and trapping see H. Metcalf and P. van der Straten, Phys. Rep. **244**, 203 (1994).

[19]R. Gupta, J. J. McClelland, Z. J. Jabbour, and R. J. Celotta, Appl. Phys. Lett. **67**, 1378 (1995); U. Drodofsky, J. Stuhler, Th. Schulze, M. Drewsen, B. Brezger, T. Pfau, and J. Mlynek, Appl. Phys. B: Lasers Opt. **65**, 755 (1997).

[20]Preliminary measurements of the period of line arrays produced by the group of J. J. McClelland and R. J. Celotta agree to within four parts in 10^4 of the expected value. J. F. Kramer (private communication).